

Energetic benefits of prey choice for a shark-eating shark

Erin T. Spencer¹, Lisa A. Hoopes², Jack J. Morris³, Demian D. Chapman³, Valerie Hagan³, Mark Johnson⁴,
Nicholas L. Payne⁵, Yuuki Y. Watanabe⁶, Ruth E. Dunn^{7,8} Yannis P. Papastamatiou¹

¹Institute of Environment, Department of Biological Sciences, Florida International University, North
Miami, FL, United States

²IUCN Center for Species Survival, Georgia Aquarium, Atlanta, GA, United States

³Sharks and Rays Conservation Program, Mote Marine Laboratory, Sarasota, FL, United States

⁴Zoophysiology, Aarhus University, Aarhus, Denmark

⁵School of Natural Sciences, Trinity College Dublin, Dublin, Ireland

⁶Research Center for Integrative Evolutionary Science, The Graduate University for Advanced Studies,
SOKENDAI, Kanagawa, Japan

⁷CNRS Centre d'Ecologie Fonctionnelle et Evolutive, CNRS, 1919 Route de Mende, Montpellier, France

⁸Lancaster Environment Centre, Lancaster University, Lancaster, U.K.

Corresponding author: Dr. Erin T. Spencer, etspencer14@gmail.com

Authors' contributions: ETS, YPP, and LAH conceived the study; ETS, JJM, DDC, VH, YYW, NLP, and YPP
completed field work; LAH and MJ provided sensors and analysis software; ETS and RED completed
analysis in R, ETS and YPP wrote the paper with contributions from all authors.

Abstract

Optimal foraging theory has been used to understand the foraging choices of animals but is rarely applied to large predatory fishes due to difficulties measuring their behavior in the wild. Great hammerhead sharks (*Sphyrna mokarran*) are atypical among sharks in that they prefer large prey, such as other sharks and large teleost species, rather than smaller teleost or invertebrate prey. Great hammerheads are known to hunt blacktip sharks (*Carcharhinus limbatus*) that form large seasonal aggregations off the coast of southern Florida. However, the foraging advantage of this dietary choice and hunting strategy is unclear. We equipped great hammerheads with biologging sensors (speed, video, sonar) to estimate swimming metabolic rates and prey encounter rates and then model the foraging benefits of hunting large prey (sharks) versus small prey (reef associated teleosts). We estimate great hammerheads need to consume 0.7% body weight (BW) per day of shark prey or 0.9 % BW per day of teleost prey. Our foraging model predicts that a ~110 kg hammerhead would only need to consume a whole ~25 kg blacktip shark once every three weeks and could survive two months during low blacktip density periods without feeding before starving to death. However, it would need to capture one to two ~1 kg teleost per day to avoid falling below its energetic baseline. Great hammerhead sharks may obtain significant benefits by hunting sharks in southern Florida, especially during the winter when prey density is high.

Keywords: Biologging, bioenergetics, foraging ecology, great hammerhead sharks

Introduction

Optimal foraging theory (OFT) provides a framework to predict animal foraging behavior based on the assumption that evolution will select behaviors that maximize an animal's net energy acquisition and overall fitness (Stephens and Krebs, 1986). Within this framework, selection of dietary items depends on prey energy content, handling time, and abundance of different prey species (Charnov,

1976). Predators are predicted to preferentially select prey based on the ratio of energy content to handling time and the abundance of more profitable prey items. Lower quality prey are predicted to only be consumed if preferred prey are scarce (Charnov, 1976; Davies, 1977; O'Donoghue et al., 1998).

Due to logistics associated with measuring parameters such as prey encounter rates in the wild, OFT predictions have been tested largely in experimental settings and with smaller animals. However, understanding the dynamics behind prey selection may be particularly important in large predators because these animals can play a significant role in regulating prey populations via consumptive and non-consumptive effects (O'Donoghue et al., 1998; Springer et al., 2003; DeLong, 2021). Understanding diet selection of predators in the wild requires measuring prey encounter rate, prey energy content, predation success, associated handling time, and the energetic costs of searching for and capturing prey (Onkonburi and Formanowicz, 1997; Stephens and Krebs, 1986; Sih and Christensen, 2001). As predators actively move in search of food, they are constantly using energy at a rate dependent on their locomotion speed. However, for pursuit predators, prey encounter rates will likely be positively related to speed and animals should select swim speeds which maximize prey encounter rates while minimizing metabolic costs (Pyke, 1981). Quantifying these parameters in large, free-ranging animals is difficult, especially for aquatic animals, that can only be observed over short periods of time (Sims and Quayle, 1998; Watanabe and Papastamatiou, 2023).

The great hammerhead shark (*Sphyrna mokarran*) is a large species (maximum total length 5 m) found in coastal and pelagic waters of tropical and temperate regions worldwide which displays long-term and seasonal residency to South Florida, USA (Guttridge et al., 2017; Gallagher and Klimley, 2018). Great hammerhead sharks are unusual among large coastal predators because their diet is dominated by other sharks and rays, with far less reliance on smaller prey, such as teleosts, crustaceans, and mollusks (Cliff, 1995; Stevens and Lyle, 1989; Chapman and Gruber, 2002; Raoult et al., 2019; Hsu et al., 2022). While most sharks consume prey <5% of their body mass (e.g. Vögler et al., 2009; Bethea et al.,

2011), great hammerhead sharks will consume prey 25% of their mass or more (e.g. Pollack et al., 2019). Observations of great hammerhead shark predation on sharks and rays have been made across their distribution (Chapman and Gruber, 2002; Mourier et al., 2013; Roemer et al., 2016), and one study found elasmobranchs were present in up to 83.2% of non-empty great hammerhead stomachs (Cliff, 1995). In southeast Florida, they are frequently observed hunting blacktip sharks (*Carcharhinus limbatus*), which aggregate in large numbers in shallow water during their annual winter migration (Kajiura and Tellman, 2016; Doan and Kajiura, 2020). Great hammerheads off Florida swim faster during the day than at night but are more likely to make stronger jerk movements (potential predatory strikes) at night potentially suggesting higher nocturnal foraging success (Spencer et al., 2025). By foraging on coastal shark species, great hammerhead sharks also act as intraguild predators and may play an especially important role in coastal food webs, as intraguild predation can affect abundance and habitat selection of mid- and low-trophic levels (Polis et al., 1989; Polis and Holt, 1992; Sitvarin and Rypstra, 2014; van Zinnicq Bergmann et al., 2024).

Great hammerhead shark diets suggest that there is a fitness advantage to consuming elasmobranch prey over smaller, easier-to-capture teleosts. Advancements in biologging technology enable the measurements of foraging behavior and energetics in large, free-ranging predators, but to date these studies have mostly been confined to marine birds and mammals (e.g. Watanabe et al., 2014; Hazen et al., 2015; Watanabe and Papastamatiou, 2023). Here we combine biologger data with biomechanical models to estimate swimming metabolic rates and daily consumption rates of great hammerhead sharks and their encounter rates with potential prey items. We then apply these estimates within an energetic framework to determine the changes in energetic status for great hammerhead sharks hunting blacktip sharks versus reef-associated teleosts. We predict that great hammerhead sharks targeting blacktip sharks will greatly reduce the overall time they spend foraging, especially during the winter when this prey is abundant.

97

98 **Materials and Methods**

99 ***Shark tagging***

100 We caught great hammerhead sharks using baited drumlines off the Gulf and Atlantic coasts of
101 Florida, United States. Drumlines had circle hooks baited with bonito (*Sarda* sp.) attached to a weight by
102 monofilament and a swivel, allowing animals to continue swimming once hooked. Once captured, great
103 hammerhead sharks were restrained alongside the boat, measured for fork length (FL), and sexed. A
104 biologging package containing a sensor that measured speed, depth, temperature, triaxial acceleration,
105 and magnetism (42 g in air, Little Leonardo, Tokyo, Japan) was attached to the shark's dorsal fin via a
106 torsion spring clamp prior to release (Chapple et al., 2015). Galvanic releases detached the float after 24
107 or 48 hours, where deployment time was determined based on weather and current conditions. All
108 Atlantic deployments were 24 hours because of the risk of being unable to recover a tag released in the
109 Gulf stream and moving a significant distance from the point of deployment (YP Papastamatiou per.
110 Obs.)

111 Speed, depth, and temperature were measured at 1 Hz. Speed sensors used factory calibrations
112 and were further tested in a swim tunnel for revised calibrations if needed. Five deployments included a
113 video logger (15 g in air, DVL400M, Little Leonardo, Tokyo, Japan) with recording duration of 8-10 hours,
114 frame rate of 30 Hz and resolution 1280 x 960 pixels. Two video tags from the Gulf of Mexico were
115 excluded because of poor visibility and a school of fish that followed the shark for the entirety of the
116 deployment (sharks 5 and 8, respectively [Table 1]). We fitted two sharks with a novel sonar recording
117 tag (200 g in air, Aarhus University, Denmark) that transmits at 1.5 MHz, has spatial resolutions of 3.9
118 mm with a range of up to 6 m in front of the animal, and a ping rate of 25 Hz (Goulet et al., 2019;
119 Tournier et al., 2021). The sonar tag provided information about organisms in the water ahead of the
120 shark regardless of water visibility or time of day (Tournier et al., 2021). Packages contained a VHF

(Advanced Telemetry Systems, Inc) and satellite transmitter (SPOT 6, Wildlife Computers, Redland WA) for package retrieval.

Speed sensor processing and bioenergetic analysis were completed in R Studio (R Core Team, version 1.2.5033, 2020). As sharks exhibit elevated swim speeds following release, we excluded the first five hours of speed data to account for recovery from capture (Iosilevskii et al., 2022). Sonar analysis was performed using MatLab (MathWorks, Inc., version r2021a) and video analysis was completed in BORIS (Friard and Gamba, 2016). Analysis of the diel changes in behavior and swim speeds by great hammerheads can be found in Spencer et al. (2025).

Bioenergetic model

We estimated swimming metabolic rates using a biomechanical model and incorporated these into an energy budget to estimate daily energetic requirements of free-swimming sharks (e.g. Dunn et al., 2022). The energy budget equation is $C=M+G+W$ where C =consumption, M =metabolism (standard and active metabolic rates and specific dynamic action [SDA, amount of energy required to digest and assimilate food]), G =growth (somatic and reproductive), and W =waste (egestion and excretion)(Lawson et al., 2020). We estimated swimming metabolic costs using a biomechanical model incorporating body mass, swim speed, and temperature (Payne et al., 2016; Iosilevskii, 2020). We calculated energy expenditure per day assuming 1 kcal = 4.2 kJ. Standard metabolic rates, or the minimum energy expenditure for basic body functions (P_0 , Mmol of ATP per second) were estimated from

$$(1) \quad P_0 = k_P m^{0.8} \exp\left(\frac{-k_T}{\tau}\right)$$

where k_P represents mmol of ATP per seconds per $\text{kg}^{0.8}$, m is the displaced mass of the shark measured in kilograms, and τ is the temperature in Kelvin (Iosilevskii et al., 2022). There is some uncertainty

around the value for k_p , so models were run with estimates between 4-5 ATP per O₂. Mass in kg (m) of all tagged individuals was determined using the weight/length relationships from fork length (FL) where (2a and b) $W = 0.00002739 * FL^{2.8046}$ and $W = 0.00000380 * FL^{3.21084}$ for male (2a) and female great hammerhead sharks (2b) (Miller et al., 2014).

Swimming metabolic rates incorporate additional energy costs required to generate motion of the animal, in addition to the standard metabolic costs. To calculate the hydrodynamic forces acting on the animal, we used established hydrodynamic formulas that have been previously applied to free swimming hammerhead sharks (Payne et al., 2016) The lift coefficient, C_L , or the dimensionless coefficient used to calculate the lift force acting on the animal, can be expressed with

$$(3) \quad C_L = \frac{\beta mg}{qS}$$

where β is the sinking factor (buoyancy), g is the acceleration of gravity (m/s²), q is dynamic pressure (pressure resulting from the flow of water), and S is the maximal cross-sectional area of the body (Payne et al., 2016; Iosilevskii, 2020).

Dynamic pressure was determined using

$$(4) \quad q = \frac{1}{2} \rho v^2$$

where ρ is water density (kg/m³) and v is animal speed (m/s). We used the average speed from each deployment to calculate dynamic pressure rather than integrating speed over time because there were times during each deployment when speed approached zero. These events, which could indicate the animal sinking for short periods of time, were infrequent but introduced large amounts of error to lift and drag coefficient calculations.

The drag coefficient, C_D , or the dimensionless coefficient used to calculate the drag force acting on the animal, can be expressed with

$$(5) \quad C_D = 0.182 + 0.0438 C_L^2$$

(Iosilevskii, 2020) and drag (D) was calculated using

168 (6)
$$D = qSC_D$$

169 Swimming metabolic rate (P, routine metabolic rate), or the cost of activity was calculated using

170 (7)
$$P = \left(P_0 + \frac{Dv}{n_m n_h e_{ATP}} \right) \frac{e_{ATP}}{n_{ATP}}$$

171 where n_m is the chemo-mechanical efficiency of the locomotive muscles (0.9), n_h is the hydrodynamic
 172 propulsion efficiency (0.75), e_{ATP} is the energy of one mmol of ATP in Joules, and n_{ATP} is the efficiency of
 173 converting a substrate to ATP (0.4) (Iosilevskii, 2020). The swimming metabolic rate formula was
 174 integrated over time to account for the effects of different temperatures and speed within each
 175 deployment.

176 Somatic growth costs were estimated based on annual growth rates for great hammerhead
 177 sharks in the Atlantic (Piercy et al., 2010). Age was estimated using a von Bertalanffy growth curve:

178 (8)
$$L_t = L_\infty (1 - e^{-k(t-t_0)})$$

179 where L_t is FL at time of tagging, L_∞ is the theoretical asymptotic FL (264.2 cm for males and 307.8 cm
 180 for females), k is the growth coefficient (0.16 for males and 0.11 for females), t_0 is the theoretical age at
 181 length zero (-1.99 for males and -2.86 for females), and t is the age at time of tagging (Piercy et al.,
 182 2010). Age at the time of tagging (t) was determined for all individuals. FL at $t + 1$ was then used to
 183 calculate the increase in body mass over a year period. Energy density of great hammerhead shark
 184 tissue has not been quantified, so we used a value of 6.07 kJ g⁻¹ based on the caloric value of scalloped
 185 hammerhead sharks (*Sphyrna lewini*) pups (Lowe, 2002) which is used in other shark energetic studies
 186 (eg. Lear et al. [2020] and Dunn et al. [2022]). Reproductive growth costs were only calculated for
 187 females, as costs were considered negligible for males and difficult to quantify. For females,
 188 reproductive costs were based on the average litter size of 15 pups born at a mass of 2.77 kg (Stevens
 189 and Lyle, 1989). We assumed the calories required per day to grow pups during gestation were
 190 consistent throughout the year.

We assumed $27 \pm 5.4\%$ of consumed energy is lost as waste based on the general estimate for fish (Brett and Groves, 1979). The cost of SDA was assumed to be $12.5 \pm 3.9\%$ of the consumed meals based on the values measured from another shark species, adult lesser spotted dogfish *Scyliorhinus canicular* (Sims and Davies, 1994). Since rates of egestion, excretion, and SDA have not been measured in adult great hammerhead sharks, we used Monte Carlo simulations to account for uncertainty.

Foraging model

We developed a Bayesian model to predict changes in the energetic state of great hammerhead sharks as they search for and capture shark and teleost prey. Our goal was to estimate how often hammerhead sharks would need to forage in the wild based on whether they are targeting shark vs teleost prey.

i) Prey encounter rate and foraging success

We calculated mean encounter rates with blacktip shark prey using individual estimates of great hammerhead shark cruising swim speeds from our biollogger deployments, and blacktip abundance data derived from aerial surveys in South Florida (Kajiura and Tellman, 2016). We used an estimate of high (winter; January – March; 288.7 ± 275.7 sharks km^{-2}) and low (summer; May – December; 5.2 ± 0.5 sharks km^{-2}) blacktip shark density (Kajiura and Tellman, 2016). We then assumed blacktips were evenly distributed at the given summer and winter densities and estimated the number of blacktips encountered per hour by a great hammerhead shark swimming in a straight line with a detection radius of 2 m. Although great hammerhead shark prey detection radii are higher than 2 m, there are many factors that affect detection range including light levels and underwater visibility (Reinero et al., 2022), and we therefore used a conservative estimate that could be compared to encounter rates based on the range of sonar and video dataloggers. We could not use biologging sensors to estimate encounter rates with blacktip sharks because great hammerhead sharks hunt blacktip sharks in shallow water very close

to shore (Doan and Kajiura, 2019), and despite our attempts, we were not able to capture sharks in those habitats.

While aerial video can detect large animals like blacktip sharks, it is ineffective for small teleosts, except in very shallow waters. To inform mean teleost prey encounter rates we used biologging data from the sonar tags deployed on the Gulf Coast of Florida and video data from cameras deployed on the Atlantic and Gulf coasts of Florida. For the sonar data we defined a teleost encounter as the presence of fish-associated swim patterns in a sonar echogram, where each echogram represents 30 seconds of a deployment (SI Figure 1). Fish-like swim patterns were only counted if they were at least two meters away from the tag to avoid including pilot fish (*Naucrates ductor*) and remoras (family Echeneidae). For the video data, we estimated the mean encounter rate of small teleost prey and identified potential prey. Whilst we deployed multiple video loggers in the Gulf of Mexico, visibility was greatly reduced in this location and most of this footage was therefore not used. Encounter rates for the Gulf and Atlantic were calculated by averaging rates from sonar and video deployments in each location.

We did not have examples of confirmed predation events on our biologging sensors, so had to use other data sources to estimate predation success. Predation success on blacktip sharks was estimated using publicly uploaded drone and cell phone videos on YouTube of great hammerhead sharks hunting sharks off the coast of Florida. We ran our model under multiple probabilities of predation success that were lower than the measured values to account for selection bias in the videos. We used different rates of predation success for blacktips and teleosts to account for the differences in size, speed, and foraging behaviors between the two prey types. There are few measures of predation success rates for large elasmobranchs on teleosts, but grey reef sharks hunting reef fish at night had predation success rates of 40% (Labourgade et al., 2020). In our model, we therefore ran teleost simulations under predation success rates of 20, 30, and 40%.

We built a Bayesian simulation model using R (R Core Team, version 1.2.5033, 2020) and JAGS (Plummer, 2003) using the “runjags” interface (Denwood, 2016) to incorporate uncertainty around estimates of prey encounter rates and calculate foraging success under scenarios where great hammerhead sharks foraged on either teleosts or blacktip sharks. Using blacktip encounter rates derived from Kajiura and Tellman (2016), teleost encounter rates from sonar and video, blacktip predation success rates derived from YouTube, and teleost success rates derived from Labourgade et al. (2020), we ran our models for seven simulations (the number of sharks with swim speed data) for four chains for 10,000 iterations, each with a burn-in of 2,000. We calculated mean encounter rates for each data stream and mean foraging success rates across the individuals within the model, thereby ensuring that uncertainties at the individual level were incorporated.

ii) *Foraging simulation model*

We constructed a foraging simulation model to compare temporal changes in energetic state as a function of prey encounter rate and predation success for foraging great hammerhead sharks when hunting two prey types and how these changed seasonally. We ran 12 models; six where we considered seasonal changes in blacktip shark densities (winter and summer, each at predation success rates of 5, 10, and 15%), and six where we considered habitat differences in reef fish encounter rates (Atlantic and Gulf of Mexico, each at predation success rates of 20, 30, and 40%). Our swimming great hammerhead sharks used energy based on the swimming metabolic rates estimated above. Rate of caloric expenditure was calculated (Equations 1-6) for two different seasonal temperature scenarios based on the average SST of a NOAA sampling site close to tagging locations in the Atlantic Coast of South Florida (29.5 °C for summer and 23.8 °C for winter). We used Monte Carlo simulations to account for variation within inputs of speed and length.

Successful predation rates for each prey item in the simulation were determined from a Poisson distribution using the average encounter rates estimated from our Bayesian model. After a successful

predation event, we assumed the entire prey item was consumed by the great hammerhead shark and 39.5% of ingested calories were lost through waste (Brett and Groves, 1979) and SDA (Sims and Davies, 1994). We used Monte Carlo simulations to estimate calories gained per predation event based on blacktip length-weight relationships, assuming a value of $6.07 \pm 1.55 \text{ kJ g}^{-1}$ (Lowe, 2002; Pollack et al., 2019). We estimate a great hammerhead would gain $22000 \pm 3200 \text{ kcal}$ for a ~25 kg blacktip. We used Malabar blood snapper (*Lutjanus malabaricus*, hereafter “snapper”) as a representative of teleost prey and caloric content was based on the length-weight relationship of an average sized individual (50 cm) (Allen, 1985; Edwards, 1985). We also assumed that if predation was successful, the shark gained approximately $665 \pm 60 \text{ kcal per kg}$ of teleost prey with a Monte Carlo simulation accounting for variation in fish size and caloric value of 4.97 kJ g^{-1} (Nurnadia et al., 2011). We ran 1000 iterations of each foraging simulation to estimate time to successful predation and great hammerhead shark energetic state following predation.

We calculated time for great hammerhead sharks to return to their energetic baseline, which we define as the number of hours between initiating foraging (time = 0) to returning to the net zero calories (calories lost from foraging plus calories gained from prey consumption). We also calculated how long a great hammerhead shark could search for prey unsuccessfully before 25% of its body mass would be consumed by its metabolism, a point beyond which we assume the animal would die of starvation (see Parsons, 1990). Values for speed, caloric estimates of each prey type, and time to predation and baselines were all expressed as mean \pm standard deviation (s.d.). This modelling was done in STELLA (ISEE Systems, version 3.5.0).

Results

Daily and yearly caloric estimates

We deployed and recovered nine biologging packages on great hammerhead sharks in Florida between February 2020 and May 2023 (Table 1). Tagged sharks ranged from 170 cm to 263 cm FL (mean 206 ± 25 cm, Table 1). There was no significant difference in average size between males and females (t-test, $p=0.9$). Almost all tagged individuals were near or above size of maturity (~ 200 cm FL [Miller et al., 2014]). Average swim speed was 0.7 ± 0.1 m/s and average individual max speed was 2.9 ± 0.8 m/s (max speed range of 1.6-3.6 m/s).

Based on our bioenergetic model, we estimate that great hammerhead sharks must consume 10 kcal per kg of body weight (BW) per day, which amounts to $0.7 \pm 0.08\%$ BW/d in shark or stingray prey, $1.3 \pm 0.1\%$ BW/d in squid prey, or $0.9 \pm 0.1\%$ BW/d in snapper prey. We estimate pregnant females must consume an additional 11 ± 3 kcal per day per pup. Assuming an average litter size of 15 pups, pregnant females must consume 12 kcal per kg of BW per day, which amounts to $0.84 \pm 0.1\%$ BW/d in shark or stingray prey, $1.5 \pm 0.2\%$ BW/d in squid prey, or $1.0 \pm 0.2\%$ BW/d in snapper prey. If females carried the maximum litter size of about 33 pups, they would need to consume 14 kcal per kg of BW per day, or $1.0 \pm 0.2\%$ BW/d in shark or stingray prey, $1.7 \pm 0.3\%$ BW/d in squid prey, or $1.2 \pm 0.2\%$ BW/d in snapper prey.

We further predict that a ~ 110 kg great hammerhead shark would require an annual consumption of 12 ± 7 blacktip sharks, assuming the entire 25 kg blacktip shark is consumed in each meal (Pollack et al., 2019), to meet measured growth rates for the Atlantic (Piercy et al., 2010). For a 10 kg stingray, great hammerhead sharks would require an annual consumption of 29 ± 13 stingrays. Great hammerhead sharks would need to consume about 1 kg of teleost prey per day or about 122 ± 44 snapper per year (based on a 3 kg average Malabar blood snapper). Pregnant females with average litters would need to consume 14 ± 7 blacktip sharks, 34 ± 14 stingrays, or 140 ± 43 snapper per year; females carrying the largest litters would need to consume 16 ± 8 blacktip sharks, 39 ± 15 stingrays, or 161 ± 44 snapper per year.

309

310 ***Prey Encounter and Predation Success Rate***

311 Blacktip encounter rate was estimated to be 3.0 ± 2.9 sharks per hour in winter and 0.5 ± 1.0
312 sharks per hour in summer. Predation success rate on blacktip sharks was determined based on 20
313 predation attempts on elasmobranchs observed across ten user-generated hammerhead hunting videos
314 on YouTube (success rates ranging from 0-33%, average 15.8% success, SI Table 1). Blacktip simulations
315 were run at 5, 10, and 15% to account for selection bias. Teleost prey encounter rate estimates were
316 based on two sonar tag deployments (both in the Gulf of Mexico) and three video tag deployments (two
317 in the Atlantic, one in the Gulf of Mexico). Video deployments had ~7-10 hours of usable daytime
318 footage per deployment, while sonar tags captured more than 30 hours of data each (Figure 1).

319 The two sonar deployments suggested average encounter rates of 8.1 ± 10.0 and 23.3 ± 30.3
320 fish per hour, respectively. The highest rate of potential prey encounter exceeded 100 in one hour for
321 shark 9, and both deployments exhibited patchiness of potential prey, with multi-hour stretches of few
322 or no encounters (Figure 1). The maximum travel time with no prey sightings was five hours in both
323 video and sonar deployments (Figure 1). The two video tag deployments in the Atlantic had a wide range
324 in potential prey encounter rates, with shark 2 and 6 exhibiting 111 and 7 encounters over 8.2 and 7.1
325 hours, respectively (Figure 1). Teleosts that could be tentatively identified in the video included fish in
326 the Lutjanidae, Serranidae, and Balistidae families (and one sighting of a dolphin and calf, see SI Figure
327 2). Our model estimated average encounter rates for potential teleost prey to be 17.5 ± 8.6 prey/hour
328 in the Gulf of Mexico and 12.1 ± 55.7 prey/hour in the Atlantic.

329

330 ***Foraging simulation model***

331 We estimated that ~2 m FL great hammerhead sharks swimming at a consistent speed of 0.7
332 ± 0.1 m/s would expend 41.1 ± 14.7 kcal/hour in summer and 35.1 ± 13 kcal/hour in winter. Without

any predation, great hammerheads are estimated to reach their energetic minimum (starvation) after about 39 days in summer and 45 days in the winter. In summer, sharks would need to forage for an average of 2.2 ± 1.0 hours before encountering a blacktip and would need to search for an average of 23.2 ± 2.0 hours, before successful capture (assuming 10% predation success rate). Great hammerhead sharks would return to their caloric baseline in 535 ± 79 hours and reach their energetic minimum after 1466 ± 79 hours, or about 61 days (Figure 2). In winter, great hammerheads encounter a blacktip in less than an hour, and predation success occurs in 3.7 ± 0.4 hours. A great hammerhead shark would return to its caloric baseline after 626 ± 92 hours, or about 26 days (Figure 2) and could swim for 1717 ± 92 hours, or about ten weeks, before reaching the energetic minimum. Even at low rates of predation success (5%), great hammerhead sharks are predicted to find and kill a blacktip in under 8 hours in winter (Table 2).

Our model predicts great hammerhead sharks could encounter and successfully consume a teleost in under 20 minutes in the Gulf of Mexico and 30 minutes in the Atlantic (assuming a 20% success predation rate, Table 2) and return to their energetic baseline in 2-3 days (Figure 2). Time to starvation following teleost predation ranged from about 40 days in the summer to 48 days in the winter.

Discussion

Optimal foraging theory predicts that animals will behave as dietary specialists or generalists based on prey energy content, handling times, foraging efficiency, and search times (Charnov, 1976; Davies, 1977). Theoretically, predators are predicted to target and specialize on prey items with the highest energy content per unit handling time, as long as search times remain below a critical level (Davies, 1977). Previous stomach content studies and stable isotope analyses of great hammerhead sharks show that their diet is dominated by sharks and rays, suggesting there is an energetic advantage

for pursuing elasmobranch prey (Cliff, 1995; Raoult et al., 2019; Lubitz et al., 2023). Here we use estimates of swimming metabolic rates and prey encounter rates derived from biologgers to show the significant advantage great hammerhead sharks obtain by hunting large prey including other sharks, rays, and larger teleost species, as opposed to much smaller teleost prey.

We estimate that great hammerhead sharks off Florida would need to consume $0.7 \pm 0.08\%$ BW/d of shark prey and $0.9 \pm 0.1\%$ BW/d in snapper prey. These estimates are lower than those of other hammerhead sharks (Lowe, 2002; Bethea et al., 2011; Heim et al., 2021). Juvenile scalloped hammerhead sharks need to consume an estimated 3.7% BW per day, but larger daily rations are expected for juveniles because they have higher mass specific metabolic rates and their diets consist of calorically poor invertebrates and teleosts (Lowe, 2002). Estimates of daily rations based on feeding behaviors of provisioned great hammerhead sharks in the Bahamas were also higher at 1.42-1.45% BW of teleosts per day, even when provisioning with teleosts that had a higher caloric content (minimum value of 5.5 kJ g^{-1} , compared to 4.97 kJ g^{-1} used in this study) (Heim et al., 2021). However, this reflects how much sharks are consuming at ecotourism sites and may indicate that sharks are being fed more than their typical daily ration during provisioning.

Our novel application of biologgers provides some of the first estimates of potential prey encounter rates in free-swimming sharks. Sonar tags showed evidence of sharks moving between patches of prey, with up to 16 hours between patch encounters (where a patch is estimated to be five or more fish) and up to five hours with no prey sightings at all. Video deployments also documented variations in prey encounters based on habitat type (sandy vs. coral/rock bottom), which indicates that time until predation success will vary between foraging location. This also ties in with our analysis of volume restricted searching by great hammerheads, which is more likely to be beneficial for teleost prey, and which is more extensively used by hammerheads on the Gulf coast of Florida where blacktip aggregations are absent (and sharks may be more likely to hunt teleosts, Spencer et al. [2025]). Sharks

likely forage in specific habitats based on time since last successful predation, or even on preferred prey type. Sonar or video tags would not necessarily record rays hidden in sandy areas, for example, and great hammerhead sharks could selectively forage in these sandy areas if seeking ray prey. Animal-borne video data did not reveal any other sharks, and our estimates of shark encounters come from aerial surveys (Kajiura and Tellman, 2016). These surveys measured blacktip shark densities in shallow water within a few hundred meters to shore where great hammerhead sharks are frequently seen patrolling, although we were not able to tag sharks in these habitats (Doan and Kajiura, 2020).

Despite the abundance of teleost prey, targeting blacktip sharks in the high-density winter months is advantageous with a great hammerhead shark having to only capture a shark about every 625 hours (26 days). However, our model suggests there are still energetic benefits for foraging on blacktips even when their densities are lower (e.g. the summer when many sharks migrate north, Bowers and Kajiura, [2025]). Even in low density periods, the energy gained from consuming a blacktip will sustain a great hammerhead shark above their energetic baseline for approximately 535 hours, or about 22 days. In summer, time to starvation was not reached until about 61 days, suggesting a great hammerhead shark could forage for an additional five to six weeks after reaching their energetic baseline. Great hammerhead sharks hunting teleosts would have to hunt and catch a fish almost daily. Based on predictions of OFT, great hammerhead sharks may only consume teleosts (or include them as a larger proportion of their diet) when blacktip abundance drops below a critical value, leading us to predict a higher proportion of smaller teleosts consumed during the summer (Davies, 1977; DeLong, 2021). Our simulation used average blacktip densities of 288 sharks per km^{-2} in winter and 5.2 sharks per km^{-2} in summer, but densities can reach peak highs of 803 sharks per km^{-2} in winter and lows of 4.2 sharks per km^{-2} in summer (Kajiura and Tellman, 2016), suggesting that the advantage of foraging for teleosts changes throughout lower density periods.

Our energetic model relies on estimates of parameters that are difficult to measure in the wild. Our estimates of prey encounter rates are based on small sample sizes due to the logistics of having to capture adult great hammerhead sharks and recover detached biologgers. Sonar and video sensors have narrow detection beams which are extended by side-to-side movement, but these sensors nevertheless may not fully cover the 2 m radius of detection used in this model. Using sight and electroreception, great hammerhead sharks can almost certainly detect much further than 2 m. We also had to use different methods to estimate prey encounter rates, due to blacktip sharks occupying very shallow habitats where we were not able to tag great hammerhead sharks. We likely overestimate blacktip shark encounters as we assume a homogeneous distribution when there is likely significant patchiness. Our blacktip shark encounter estimates do not account for behavioral responses by blacktips to great hammerhead sharks, where they rapidly swim into very shallow water and will disperse (Brown et al., 1999; Doan and Kajiura, 2020). For example, information on an approaching hammerhead shark will likely spread rapidly throughout the blacktip aggregation causing all individuals to move to shallower water and reducing predation success (Papastamatiou et al., 2022). Simulations do not include estimates of handling time because there is limited data for great hammerhead shark prey. Published estimates of handling of stingrays ranges from 10 to more than 25 minutes (Strong et al., 1990; Chapman and Gruber, 2002). Great hammerhead sharks will almost certainly be digestion limited after consuming an entire blacktip shark, although we would expect gastric evacuation times of 1-2 days (Wetherbee et al. 1990). Additionally, consumption of large prey may lead to losses from kleptoparasitism with competitors and increases the risk of injury to predators (hammerheads) from the prey themselves (Berger-Tal et al., 2009; Mukherjee and Heithaus, 2013). Finally, our model relies on parameters that are impossible to collect using one biologging method, resulting in our having to combine multiple methods to estimate encounter rate and predation success. We used a Bayesian model to account for uncertainty resulting from multiple data inputs and stabilize inferences from a relatively small sample sizes, and

although we acknowledge this approach still introduces potential biases and assumptions, our findings still provide valuable estimates that support behavioral observations and can guide future ecological models.

Despite these assumptions within our model, we show that great hammerhead sharks hunting other sharks is more energetically profitable than hunting teleosts. The energetic advantage gained by foraging on large prey may explain why great hammerhead sharks regularly consume prey at least 25% of their own body mass. As intraguild predators (both hammerheads and their blacktip prey also consume teleost prey) great hammerheads may have wider ecological impacts through their impacts on habitat selection of their intraguild prey (blacktip sharks) and shared resource (teleosts etc., van Zinnicq Bergmann et al. [2024]). OFT further predicts that changes in the abundance of preferred prey items will cause dietary switches with profound ecological implications for some marine species (e.g. Springer et al., 2003). Understanding the energetic foraging costs of ectothermic marine predators and the consequences of prey choice is especially critical as global climate change continues to alter the ranges of both predator and prey species (Osgood et al., 2021). The blacktip shark migration in southeast Florida is highly correlated with temperature, and warming could shift the migration northward, which could reduce seasonal prey availability for top predators like great hammerhead sharks (Kajiura and Tellman, 2016; Bowers and Kajiura, 2025). Higher metabolic costs in warmer water and lower abundance of preferred prey could also result in changes in foraging rates, distribution, or diet for great hammerhead sharks with important population-level consequences.

Acknowledgements: We would like to thank K. Gastrich, B. Binder, C. Fields, L. Garcia Barcia, S. Casareto, S. Schoen, M. Kelly, K. Flowers, S. Luongo, D. Butkowski, the ANGARI Crew, and many others at FIU and Mote Marine Lab for their assistance in the field. We thank G. Iosilevskii for his support in data

analysis. This is contribution #1994 from the Coastlines and Oceans Division of the Institute of Environment at Florida International University.

Funding: This study was conducted with primary financial support from Georgia Aquarium. Additional funding was provided by the FIU Graduate School, FIU Institute of the Environment, and the Explorers Club. Additional field support was provided by BBC, National Geographic, OceanX, ANGARI Foundation, and Mote Marine Lab.

Conflict of interest: The authors declare that they have no conflict of interest.

Ethics approval: All applicable institutional and/or national guidelines for the care and use of animals were followed. Shark tagging was approved by FIU IACUC #201480.

Consent for publication: N/A

Availability of data and material: The data used during the current study are available from the corresponding author on reasonable request.

Code availability: Speed sensor processing and bioenergetic analysis were completed with custom code in R Studio (R Core Team, version 1.2.5033, 2020). Sonar analysis was performed with custom code in MatLab (MathWorks, Inc., version r2021a) and video analysis was completed in BORIS (Friard and Gamba, 2016).

Authors' contributions: ETS, YPP, and LAH conceived the study; ETS, JJM, DDC, VH, YYW, NLP, and YPP completed field work; LAH and MJ provided sensors and analysis software; ETS and RED completed analysis in R, ETS and YPP wrote the paper with contributions from all authors.

Works Cited

Allen, G. (1985). *FAO Species Catalogue: Vol. 6. Snappers of the World. FAO Fisheries Synopsis* (Vol. 6).

473 Berger-Tal, O., Mukherjee, S., Kotler, B. P., & Brown, J. S. (2009). Look before you leap: Is risk of injury a
 474 foraging cost? *Behavioral Ecology and Sociobiology*, 63(12), 1821–1827.
 475 <https://doi.org/10.1007/s00265-009-0809-3>

476 Bethea, D. M., Carlson, J. K., Hollensead, L. D., Papastamatiou, Y. P., & Graham, B. S. (2011). A
 477 comparison of the foraging ecology and bioenergetics of the early life-stages of two sympatric
 478 hammerhead sharks. *Bulletin of Marine Science*, 87(4), 873–889.
 479 <https://doi.org/10.5343/bms.2010.1047>

480 Bowers, M.E., Kajiura, S.M. (2025). Seasonal distribution and environmental predictors of the
 481 movement of male blacktip sharks *Carcharhinus limbatus* off the US East Coast. *Marine*
 482 *Ecology Progress Series*. 753, 119-135

483 Brett, J.R. & Groves, T.D.D. (1979). Physiological energetics. In W.S. Hoar; D.J. Randall & J.R. Brett, (Eds.),
 484 *Fish Physiology, VIII: Bioenergetics and Growth* (pp. 279-352). New York: Academic Press.

485 Brown, J. S., Laundré, J. W., & Gurung, M. (1999). The ecology of fear: Optimal foraging, game theory,
 486 and trophic interactions. *Journal of Mammalogy*, 80(2), 385–399.

487 Chapman, D. D., & Gruber, S. H. (2002). A further observation of the prey-handling behavior of the great
 488 hammerhead shark, *Sphyrna mokarran*: Predation upon the spotted eagle ray, *Aetobatus narinari*.
 489 *Bulletin of Marine Science*, 70(3), 947–952. <https://api.semanticscholar.org/CorpusID:82921408>

490 Chapple, T. K., Gleiss, A. C., Jewell, O. J. D., Wikelski, M., & Block, B. A. (2015). Tracking sharks without
 491 teeth: A non-invasive rigid tag attachment for large predatory sharks. *Animal Biotelemetry*, 3(14).
 492 <https://doi.org/10.1186/s40317-015-0044-9>

493 Charnov, E. L. (1976). Optimal foraging: Attack strategy of a mantid. *The American Naturalist*, 110(971),
 494 141–151. <https://www.jstor.org/stable/2459883>

495 Cliff, G. (1995). Sharks caught in the protective gill nets off KwaZulu-Natal, South Africa. 8. The great
 496 hammerhead shark *Sphyrna mokarran* (Rüppell). *South African Journal of Marine Science*, 15(1),
 497 105–114. <https://doi.org/10.2989/025776195784156331>

498 Davies, N. B. (1977). Prey selection and the search strategy of the spotted flycatcher (*Muscicapa striata*):
 499 A field study on optimal foraging. *Animal Behaviour*, 25, 1016–1033. [https://doi.org/10.1016/0003-](https://doi.org/10.1016/0003-3472(77)90053-7)
 500 [3472\(77\)90053-7](https://doi.org/10.1016/0003-3472(77)90053-7)

501 DeLong, J. P. (2021). Predator Ecology: Evolutionary Ecology of the Functional Response. New York, NY:
 502 Oxford University Press.

503 Denwood, M. J. (2016). runjags: An R package providing interface utilities, model templates, parallel
 504 computing methods and additional distributions for MCMC models in JAGS. *Journal of Statistical*
 505 *Software*, 71(9). <https://doi.org/10.18637/jss.v071.i09>

506 Doan, M. D., & Kajiura, S. M. (2020). Adult blacktip sharks (*Carcharhinus limbatus*) use shallow water as
 507 a refuge from great hammerheads (*Sphyrna mokarran*). *Journal of Fish Biology*, 96, 1530–1533.
 508 <https://doi.org/10.1111/jfb.14342>

509 Edwards, R. R. C. (1985). Growth rates of Lutjanidae (snappers) in tropical Australian waters. *Journal of*
 510 *Fish Biology*, 26(1), 1–4. <https://doi.org/10.1111/j.1095-8649.1985.tb04233.x>

511 Friard, O., & Gamba, M. (2016). BORIS: A free, versatile open-source event-logging software for
 512 video/audio coding and live observations. *Methods in Ecology and Evolution*, 7, 1325–1330.
 513 <https://doi.org/10.1111/2041-210X.12584>

514 Gallagher, A. J., & Klimley, A. P. (2018). The biology and conservation status of the large hammerhead
 515 shark complex: The great, scalloped, and smooth hammerheads. *Reviews in Fish Biology and*
 516 *Fisheries*, 28(4), 777–794. <https://doi.org/10.1007/s11160-018-9530-5>

517 Goulet, P., Guinet, C., Swift, R., Madsen, P. T., & Johnson, M. (2019). A miniature biomimetic sonar and
 518 movement tag to study the biotic environment and predator-prey interactions in aquatic animals.
 519 *Deep-Sea Research Part I*, 148, 1–11. <https://doi.org/10.1016/j.dsr.2019.04.007>

520 Guttridge, T. L., Van Zinnicq Bergmann, M. P. M., Bolte, C., Howey, L. A., Finger, J. S., Kessel, S. T.,
 521 Brooks, J. L., Winram, W., Bond, M. E., Jordan, L. K. B., Cashman, R. C., Tolentino, E. R., Grubbs, D.
 522 R., & Gruber, S. H. (2017). Philopatry and regional connectivity of the great hammerhead shark,
 523 *Sphyrna mokarran* in the U.S. and Bahamas. *Frontiers in Marine Science*, 4, 1–15.
 524 <https://doi.org/10.3389/fmars.2017.00003>

525 Hazen, E. L., Friedlaender, A. S., & Goldbogen, J. A. (2015). Blue whales (*Balaenoptera musculus*)
 526 optimize foraging efficiency by balancing oxygen use and energy gain as a function of prey density.
 527 *Science Advances*, 1(9). <https://doi.org/10.1126/sciadv.1500469>

528 Heim, V., Dhellemmes, F., Smukall, M. J., Gruber, S. H., & Guttridge, T. L. (2021). Effects of food
 529 provisioning on the daily ration and dive site use of great hammerhead sharks, *Sphyrna mokarran*.
 530 *Frontiers in Marine Science*, 8. <https://doi.org/10.3389/fmars.2021.628469>

531 Hsu, H. H., Nazeer, Z., Panickan, P., Lin, Y. J., Qasem, A., Rabaoui, L. J., & Qurban, M. A. (2022). Stomach
 532 content analysis for juvenile great hammerhead sharks *Sphyrna mokarran* (Rüppell, 1837) from the
 533 Arabian Gulf. *Fishes*, 7(6). <https://doi.org/10.3390/fishes7060359>

534 Iosilevskii, G. (2020). Centre-of-mass and minimal speed limits of the great hammerhead. *Royal Society*
 535 *Open Science*, 7(10). <https://doi.org/10.1098/rsos.200864>

536 Iosilevskii, G., Kong, J. D., Meyer, C. G., Watanabe, Y. Y., Papastamatiou, Y. P., Royer, M. A., Nakamura, I.,
 537 Sato, K., Doyle, T. K., Harman, L., Houghton, J. D.R., Barnett, A., Semmens, J. M., Maoiléidigh, N.
 538 O., Drumm, A., O'Neill, R., Coffey, D. M., & Payne, N. L. (2022). A general swimming response in
 539 exhausted obligate swimming fish. *Royal Society Open Science*, 9(9).
 540 <https://doi.org/10.1098/rsos.211869>

541 Kajiura, S. M., & Tellman, S. L. (2016). Quantification of massive seasonal aggregations of blacktip sharks
 542 (*Carcharhinus limbatus*) in southeast Florida. *PLoS ONE*, 11(3), 1–16.
 543 <https://doi.org/10.1371/journal.pone.0150911>

544 Labourgade, P., Ballesta, L., Huveneers, C., Papastamatiou, Y., & Mourier, J. (2020). Heterospecific
 545 foraging associations between reef-associated sharks: First evidence of kleptoparasitism in sharks.
 546 *Ecology*, 101(11), 1–4. <https://doi.org/10.1002/ecy.3117>

547 Lawson, C. L., Halsey, L. G., Hays, G. C., Dudgeon, C. L., Payne, N. L., Bennett, M. B., White, C. R., &
 548 Richardson, A. J. (2019). Powering ocean giants: The energetics of shark and ray megafauna. *Trends*
 549 *in Ecology and Evolution*, 34(11), 1009–1021. <https://doi.org/10.1016/j.tree.2019.07.001>

550 Lowe, C. G. (2002). Bioenergetics of free-ranging juvenile scalloped hammerhead sharks (*Sphyrna lewini*)
 551 in Kane’ohe Bay, O’ahu, HI. *Journal of Experimental Marine Biology and Ecology*, 278, 141–156.
 552 [https://doi.org/10.1016/S0022-0981\(02\)00331-3](https://doi.org/10.1016/S0022-0981(02)00331-3)

553 Lubitz, N., Abrantes, K., Crook, K., Currey-Randall, L. M., Chin, A., Sheaves, M., Fitzpatrick, R., Martins, A.
 554 B., Bierwagen, S., Miller, I. B., Barnett, A. (2023). Trophic ecology shapes spatial ecology of two
 555 sympatric predators, the great hammerhead shark (*Sphyrna mokarran*) and bull shark
 556 (*Carcharhinus leucas*). *Frontiers in Marine Science*, 10.
 557 <https://doi.org/10.3389/fmars.2023.1274275>

558 Miller, M. H., Carlson, J., Hogan, L., & Kobayashi, D. (2014). *Status review report: Great hammerhead*
 559 *shark* (*Sphyrna mokarran*). Final Report to National Marine Fisheries Service, Office of Protected
 560 Resources. 116 pp. <https://repository.library.noaa.gov/view/noaa/16286>

561 Mourier, J., Planes, S., & Buray, N. (2013). Trophic interactions at the top of the coral reef food chain.
 562 *Coral Reefs*, 32, 285. <https://doi.org/10.1007/s00338-012-0976-y>

563 Mukherjee, S., & Heithaus, M. R. (2013). Dangerous prey and daring predators: A review. *Biological*
 564 *Reviews*, 88(3), 550–563. <https://doi.org/10.1111/brv.12014>

565 Nurnadia, A. A., Azrina, A., & Amin, I. (2011). Proximate composition and energetic value of selected
 566 marine fish and shellfish from the West Coast of Peninsular Malaysia. *International Food Research*
 567 *Journal*, 18, 137–148.

568 O’Donoghue, M., Boutin, S., Krebs, C. J., Zuleta, G., Murray, D. L., & Hofer, E. J. (1998). Functional
 569 responses of coyotes and lynx to the snowshoe hare cycle. *Ecology*, 79(4), 1193–1208.
 570 <https://doi.org/10.2307/3546927>

571 Onkonburi, J., & Formanowicz, D. R. (1997). Prey choice by predators: Effect of prey vulnerability.
 572 *Ethology Ecology and Evolution*, 9(1), 19–25. <https://doi.org/10.1080/08927014.1997.9522899>

573 Osgood, G. J., White, E. R., & Baum, J. K. (2021). Effects of climate-change-driven gradual and acute
 574 temperature changes on shark and ray species. *Journal of Animal Ecology*, 90(11), 2547–2559.
 575 <https://doi.org/10.1111/1365-2656.13560>

576 Papastamatiou, Y.P., Mourier, J., Vila Pouca, C., Guttridge, T.L., Jacoby, D.M.P. (2022). Shark and ray
 577 social lives: form, function, and ecological significance of associations and grouping. *In* Biology of
 578 Sharks and their relatives 3rd edition (eds. Carrier, J.C., Simpfendorfer, C.A., Heithaus, M.R., Yopak,
 579 K.E). CRC Press. 545-566

580 Parsons, G. R. (1990). Metabolism and swimming efficiency of the bonnethead shark *Sphyrna tiburo*.
 581 *Marine Biology*, 104, 363–367. <https://doi.org/10.1007/BF01314338>

582 Payne, N. L., Iosilevskii, G., Barnett, A., Fischer, C., Graham, R. T., Gleiss, A. C., & Watanabe, Y. Y. (2016).
 583 Great hammerhead sharks swim on their side to reduce transport costs. *Nature Communications*,
 584 7, 6–10. <https://doi.org/10.1038/ncomms12289>

585 Piercy, A. N., Carlson, J. K., & Passerotti, M. S. (2010). Age and growth of the great hammerhead shark,
 586 *Sphyrna mokarran*, in the north-western Atlantic Ocean and Gulf of Mexico. *Marine and*
 587 *Freshwater Research*, 61, 992–998. <https://doi.org/10.1071/MF09227>

588 Plummer, M. (2003). JAGS: A program for analysis of Bayesian graphical models using Gibbs sampling.
 589 *Proceedings of the 3rd International Conference on Distributed Statistical Computing*, 1–10.
 590 Retrieved from <http://www.ci.tuwien.ac.at/Conferences/DSC-2003/>

591 Polis, G. A., Myers, C. A., & Holt, R. D. (1989). The ecology and evolution of intraguild predation:
 592 Potential competitors that eat each other. *Annual Review of Ecology and Systematics*, 20, 297–330.
 593 <https://doi.org/10.1146/annurev.es.20.110189.001501>

594 Polis, G. A., & Holt, R. D. (1992). Intraguild predation: The dynamics of complex trophic interactions.
 595 *Trends in Ecology & Evolution*, 7(5), 151–154. [https://doi.org/10.1016/0169-5347\(92\)90208-S](https://doi.org/10.1016/0169-5347(92)90208-S)

596 Pollack, A. G., Driggers III, W. B., Hanisko, D. S., & Ingram, G. W. (2019). *Distribution and Length Data for*
 597 *Blacktip Sharks Captured on the NOAA / NMFS / SEFSC / MSLABS Bottom Longline Survey in the*
 598 *Western North Atlantic Ocean*. SEDAR65-DW15. SEDAR, North Charleston, S.C.

599 Pyke, G. H. (1981). Optimal travel speeds of animals. *The American Naturalist*, 118(4), 475–
 600 487. <https://doi.org/10.1086/283842>

601 R Core Team (2020). R: A language and environment for statistical computing. R Foundation for
 602 Statistical Computing, Vienna, Austria. URL <https://www.R-project.org/>.

603

604 Raoult, V., Broadhurst, M. K., Peddemors, V. M., Williamson, J. E., & Gaston, T. F. (2019). Resource use of
 605 great hammerhead sharks (*Sphyrna mokarran*) off eastern Australia. *Journal of Fish Biology*,
 606 95(6), 1430–1440. <https://doi.org/10.1111/jfb.14160>

607 Reinero, F. R., Sperone, E., Giglio, G., Pacifico, A., Mahrer, M., & Micarelli, P. (2022). Influence of
 608 environmental factors on prey discrimination of bait-attracted white sharks from Gansbaai, South
 609 Africa. *Animals*, 12(23), 1–13. <https://doi.org/10.3390/ani12233276>

610 Roemer, R. P., Gallagher, A. J., Hammerschlag, N., Roemer, R. P., Gallagher, A. J., & Shallow, N. H. (2016).
 611 Shallow water tidal flat use and associated specialized foraging behavior of the great hammerhead

612 shark (*Sphyrna mokarran*). *Marine and Freshwater Behaviour and Physiology*, 49(4), 235-249.

613 <https://doi.org/10.1080/10236244.2016.1168089>

614 Shelden, K. E. W., Rugh, D. J., Mahoney, B. A., & Dahlheim, M. E. (2003). Killer whale predation on

615 belugas in Cook Inlet, Alaska: Implications for a depleted population. *Marine Mammal Science*,

616 19(3), 529–544. <https://doi.org/10.1111/j.1748-7692.2003.tb01319.x>

617 Sih, A., & Christensen, B. (2001). Optimal diet theory: When does it work, and when and why does it fail?

618 *Animal Behaviour*, 61(2), 379–390. <https://doi.org/10.1006/anbe.2000.1592>

619 Sims, D.W., & Davies, S.J. (1994). Does specific dynamic action (SDA) regulate return of appetite in the

620 lesser spotted dogfish, *Scyliorhinus canicula*? *Journal of Fish Biology*, 45(2), 341–348.

621 <https://doi.org/10.1111/j.1095-8649.1994.tb01313.x>

622 Sims, D.W., & Quayle, V.A. (1998). Selective foraging behavior of basking sharks on zooplankton in a

623 small-scale front. *Nature*, 393, 460-464. <https://doi.org/10.1038/30959>

624 Sitvarin, M. I., & Rypstra, A. L. (2014). The importance of intraguild predation in predicting emergent

625 multiple predator effects. *Ecology*, 95(10), 2946–2952. <https://doi.org/10.1890/13-2347.1>

626 Spencer, E. T., Hoopes, L.A., Morris, J.J., Chapman, D.D., Hagan, V., Papastamatiou, Y.P. (2025).

627 Searching day and night: diel hierarchical search patterns in a large marine predator that never

628 stops swimming. *Animal Behaviour*. In Press

629 Springer, A. M., Estes, J. A., Van Vliet, G. B., Williams, T. M., Doak, D. F., Danner, E. M., Forney, K. A.,

630 Pfister, B. (2003). Sequential megafaunal collapse in the North Pacific Ocean: An ongoing legacy of

631 industrial whaling? *Proceedings of the National Academy of Sciences of the United States of*
632 *America*, 100(21), 12223–12228. <https://doi.org/10.1073/pnas.1635156100>

633 Stephens, D. W., & Krebs, J. R. (1986). Foraging theory. Princeton, NJ: Princeton University Press.

634 Stevens, J. D., & Lyle, J. M. (1989). Biology of three hammerhead sharks (*Eusphyra blochii*, *Sphyrna*
635 *mokarran* and *S. lewini*) from Northern Australia. *Australian Journal of Marine and Freshwater*
636 *Research*, 40(2), 46–129. <https://doi.org/10.1071/MF9890129>

637 Strong, W. R., Snelson, F. F., & Gruber, S. H. (1990). Hammerhead shark predation on stingrays: An
638 observation of prey handling by *Sphyrna mokarran*. *Copeia*, 1990(3), 836–840.
639 <https://doi.org/10.2307/1446449>

640 Tournier, M., Goulet, P., Fonvieille, N., Nerini, D., Johnson, M., & Guinet, C. (2021). A novel animal-borne
641 miniature echosounder to observe the distribution and migration patterns of intermediate trophic
642 levels in the Southern Ocean. *Journal of Marine Systems*, 223.
643 <https://doi.org/10.1016/j.jmarsys.2021.103608>

644 van Zinnicq Bermann, M.P.M, Griffin, L.P., Bodey, T.W., Guttridge, T.L., Aarts, G., Heithaus,
645 M.R., Smukall, M.J., Papastamatiou, Y.P. (2024). Intraguild processes drive space-use
646 patterns in a large-bodied marine predator community. *Journal of Animal Ecology*. 93:876-
647 890

648 Vögler, R., Milessi, A. C., & Duarte, L. O. (2009). Changes in trophic level of *Squatina guggenheim* with
649 increasing body length: Relationships with type, size, and trophic level of its prey. *Environmental*
650 *Biology of Fishes*, 84(1), 41–52. <https://doi.org/10.1007/s10641-008-9387-x>

- 651 Watanabe, Y. Y., Ito, M., & Takahashi, A. (2014). Testing optimal foraging theory in a penguin–krill
652 system. *Proceedings of the Royal Society B: Biological Sciences*, 281(1779).
653 <https://doi.org/10.1098/rspb.2013.2376>
- 654 Watanabe, Y. Y., & Papastamatiou, Y. P. (2023). Biologging and biotelemetry: Tools for understanding
655 the lives and environments of marine animals. *Annual Review of Animal Biosciences*, 11, 247–267.
656 <https://doi.org/10.1146/annurev-animal-050322-073657>
- 657 Wetherbee, B.M., Gruber, S., Cortes, E. (1990). Diet, feeding habits, digestion and consumption in sharks
658 with special references to the lemon shark *Negaprion brevirostris*. In *Elasmobranchs as Living*
659 *Resources: Advances in the biology, ecology, systematics and the status of the fisheries* (ed. Pratt
660 H, Gruber S, Taniuchi T). NOAA Technical report 90:29-47

661

Table 1

Shark #	Location	Date (DD-Month-YY)	Duration (hrs)	FL (cm)	Avg Speed (m/s)	Sex	Data collected
1	Miami, FL (Atl)	17-Feb-2020	20.4	197	0.62 (\pm 0.1)	F	S, T, D
2	West Palm, FL (Atl)	11-Feb-2021	13.6	198	0.74 (\pm 0.1)	F	S, T, D, V
3	West Palm, FL (Atl)	12-Feb-2021	14.5	204	0.86 (\pm 0.2)	M	S, T, D
4	Sarasota, FL (Gulf)	27-Apr-2021	15.2	199	0.63 (\pm 0.3)	F	S, T, D, V
5	Sarasota, FL (Gulf)	11-May-2021	34.6	170	NA	F	T, D, V*
6	West Palm, FL (Atl)	2-Apr-2022	15.5	254	0.60 (\pm 0.2)	M	S, T, D, V
7	Sarasota, FL (Gulf)	25-Apr-2022	34.0	175	0.67 (\pm 0.2)	M	S, T, D, So
8	Sarasota, FL (Gulf)	26-Apr-2022	35.4	218	0.83(\pm 0.2)	F	S, T, D, V*
9	Sarasota, FL (Gulf)	25-Apr-2023	36.7	263	NA	F	T, D, So

Details of biologgers deployed on great hammerhead sharks. Sensors include S = Speed, T =

Temperature, D = Depth, V=video, and So = Sonar. Whether animals were tagged in the Gulf of Mexico or the Atlantic is indicated in the Location column with “Gulf” or “Atl,” respectively. In two deployments (Shark 5 and 8), the sensors failed to collect speed data and were therefore not included in calculations for average speed.

Table 2

Simulation type	Time to predation (5% success) (h)	Time to predation (10% success) (h)	Time to predation (15% success) (h)
Blacktip summer	42.16 (± 3.58)	23.16 (± 2.05)	14.68 (± 1.16)
Blacktip winter	7.12 (± 0.55)	3.67 (± 0.26)	2.43 (± 0.24)
	Time to predation (20% success) (h)	Time to predation (30% success) (h)	Time to predation (40% success) (h)
Teleost Gulf	0.30 (± 0.03)	0.19 (± 0.01)	0.14 (± 0.02)
Teleost Atlantic	0.40 (± 0.05)	0.27 (± 0.02)	0.20 (± 0.01)

Foraging simulation results for time to predation success. Results are written as mean (\pm SD).

Figure Legends

Figure 1: Example biologging data from great hammerheads, including a) speed and depth from shark 3 (Table 1) (n=1); potential prey encounters based on b) sonar tag deployments (n=2) and c) video deployments (n=3). The green line in panel c) indicates where the deployment for 2 and 6 ended (~7 hours)

Figure 2: Foraging simulations predicting changes in non-pregnant great hammerhead shark energetic state when hunting two prey types: blacktip sharks in the summer and winter (assuming 10% success) and teleosts in the summer (assuming 30% success). Kcal from baseline represents caloric gain or loss from the time the animal initiates foraging (t=0). Shading represents 95% CI around calories gained per prey item. Teleost capture time in Gulf of Mexico and Atlantic simulations varied by <10 min but results here are for foraging in the Gulf of Mexico. 95% CIs are as follows: Blacktip summer (95% CI: 23.0 to 23.3 hours); blacktip winter (95% CI: 3.6 to 3.7 hours); teleost in the Gulf of Mexico (95% CI: 11.3 to 11.4 minutes)

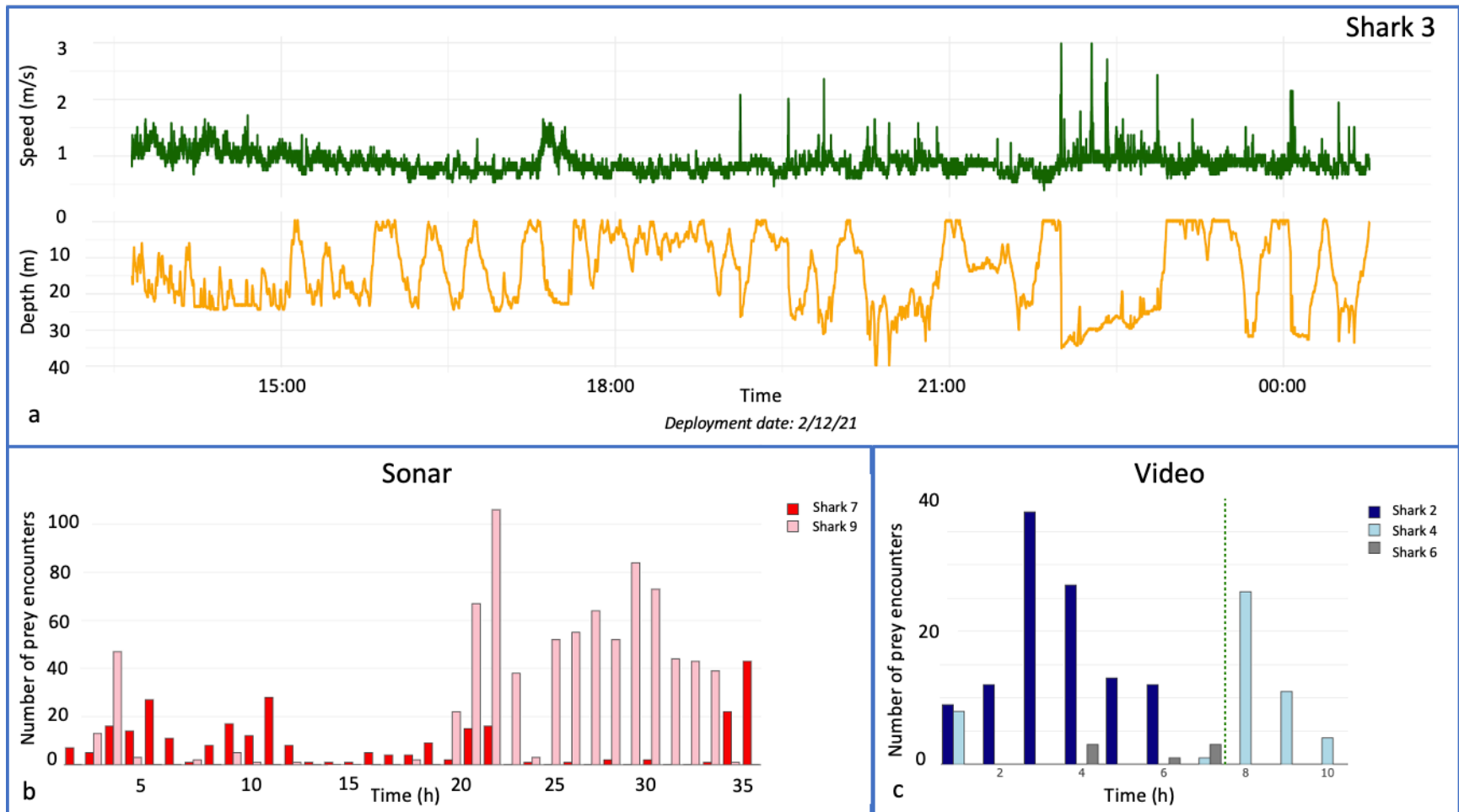


Figure 1

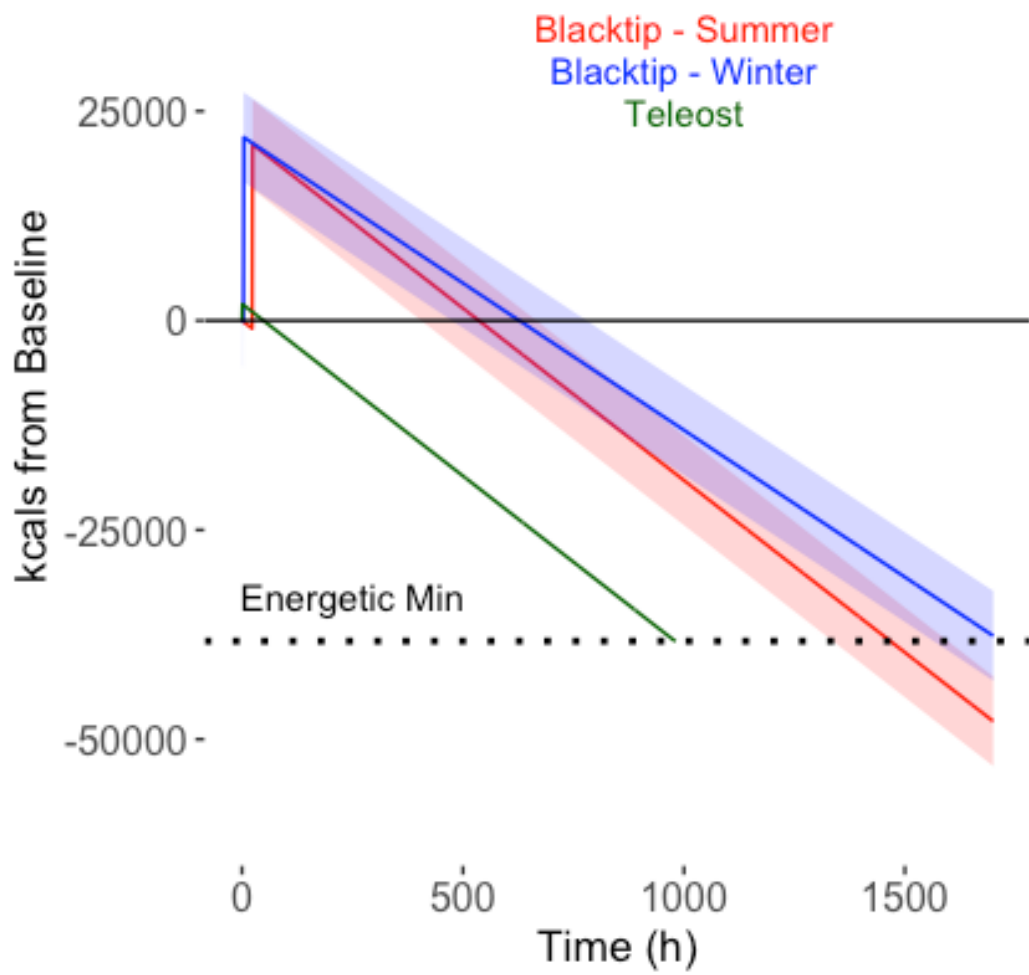


Figure 2